

kinetics of the termination reaction and places in a truer perspective the relative contributions of end and random initiation of volatile formation. But possibly the most interesting feature of this work is the difference it reveals between thermal (radical) and anionic polystyrenes. This provides strong circumstantial evidence for the existence of labile structures within the backbone of the former. When considered alongside evidence from earlier comparative studies of such polymers, we believe that the case for weak links in radical polystyrenes is satisfactorily proven.

**Acknowledgment.** Helpful discussions with Dr. L. Batt are gratefully acknowledged.

## References and Notes

- (1) (a) University of Aberdeen; (b) Robert Gordon's Institute of Technology.
- (2) G. G. Cameron, *Makromol. Chem.*, **100**, 255 (1967).
- (3) (a) G. G. Cameron and G. P. Kerr, *Eur. Polym. J.*, **4**, 709 (1968); (b) *ibid.*, **6**, 423, (1970).
- (4) G. G. Cameron and I. T. McWalter, *Eur. Polym. J.*, **6**, 1601 (1970).
- (5) L. A. Wall, S. Straus, R. E. Florin, and L. J. Fetters, *J. Res. Natl. Bur. Stand., Sect. A*, **77**, 157 (1973).
- (6) L. A. Wall, S. Straus, J. H. Flynn, D. McIntyre, and R. Simha, *J. Phys. Chem.*, **70**, 53 (1966).
- (7) D. H. Richards and L. A. Salter, *Polymer*, **8**, 153 (1967).
- (8) M. Gordon, *Trans. Faraday Soc.*, **54**, 1345 (1958).
- (9) R. H. Boyd, *J. Chem. Phys.*, **31**, 321 (1959).
- (10) R. H. Boyd, *J. Polym. Sci., Part A-1*, **5**, 1373 (1967).
- (11) N. Grassie and W. W. Kerr, *Trans. Faraday Soc.*, **53**, 234 (1956); **55**, 1050 (1959).
- (12) F. R. Mayo, *J. Am. Chem. Soc.*, **90**, 1289 (1968).
- (13) K. Buchholz and K. Kirchner, *Makromol. Chem.*, **177**, 935 (1976).
- (14) H. F. Kauffmann, O. F. Olaj, and J. W. Breitenbach, *Makromol. Chem.*, **177**, 939 (1976).
- (15) O. F. Olaj, *Monatsh. Chem.*, **102**, 648 (1971).
- (16) O. F. Olaj, H. F. Kauffmann, and J. W. Breitenbach, *J. Polym. Sci., Polym. Lett. Ed.*, **15**, 229 (1977).
- (17) By comparison with Figure 11 of ref 5 and with data on the same polymers published in ref 6 it can be established that the ordinate scale on Figure 6 of ref 5 should read  $(dC/dt) \times 10 \text{ min}^{-1}$ .
- (18) A. Nakajima, F. Hamada, and T. Shimizu, *Makromol. Chem.*, **90**, 229 (1966).
- (19) I. T. McWalter, Ph.D. Thesis, University of Aberdeen, 1977.
- (20) L. A. Wall, S. Straus, and L. J. Fetters, *Polym. Prepr. Am. Chem. Soc., Div. Polym. Chem.*, **10** (2), 1472 (1969).

## Methyl Group Tunneling and Viscoelastic Relaxation in Poly(methyl methacrylate)<sup>1</sup>

J. Williams and A. Eisenberg\*

Department of Chemistry, McGill University,  
Montreal, Quebec, Canada H3A 2K6. Received October 25, 1977

**ABSTRACT:** This paper describes a dynamic mechanical investigation of the backbone methyl relaxation in poly(methyl methacrylate) (PMMA); the normal and fully deuterated polymers were studied by high precision torsional pendulum, vibrating reed, and ultrasonic techniques in the temperature region of ca.  $-200$  to  $+50$  °C. Two very small relaxations were observed in the backbone methyl region of free-radically prepared PMMA and interpreted as due to motions of backbone methyls corresponding to syndiotactic and heterotactic main chain configurations. Evidence of quantum mechanical tunneling was present for the syndiotactic methyl relaxation, which showed not only pronounced curvature in the  $\log \nu$  vs.  $1/T$  plot at low frequencies but also a large isotope effect, with the linearity in the  $\log \nu$  vs.  $1/T$  plot for fully deuterated PMMA continuing to a much lower frequency than that for the nondeuterated polymer. Both of these effects have been predicted from theoretical considerations and have now been verified experimentally. This is the first observation of an isotope effect in the field of polymer mechanical properties. When the present data for the backbone methyl relaxations together with literature data for the glass transition, ester side group, and "water" dispersions in PMMA were extrapolated to high temperatures, the relaxations all appeared to converge in a frequency/temperature region near  $\log \nu \sim 9$  and  $T \sim 200$  °C.

## I. Introduction

**A. Development of the Quantum Mechanical Tunneling Hypothesis for Methyl Group Motions in Solids.** Methyl group motions in methyl-containing solids have long been investigated by various experimental techniques, especially proton NMR methods such as spin-lattice relaxation, line width, and second moment studies.<sup>2</sup> As the temperature is lowered, minima in the spin-lattice relaxation time and increases in line width and second moment occur, corresponding to freezing-in of methyl motion. In each type of experiment, a frequency  $\nu$  may be associated with the motion<sup>3</sup> and correlated with the temperature. In this way frequency-temperature relationships can be established for particular methyl group motions.

The temperature dependence of group motions such as barrier hopping of various side chains including methyl groups has, in the past, frequently been expressed by an Arrhenius equation, which may be written as:<sup>4</sup>

$$\nu = \nu_0 e^{-E/RT} \quad (1)$$

where  $T$  is the absolute temperature and  $E$  is the energy barrier restricting the motion of the group. Here,  $\nu_0$  is the frequency corresponding to infinite temperature, for which a value of  $10^{13}$  Hz has been suggested.<sup>5</sup> This equation predicts a straight line relationship between  $\log \nu$  and  $1/T$  with the slope proportional to the barrier height  $E$ .

Low-temperature NMR tests on methyl-containing solids have not, however, shown an Arrhenius type of behavior. This can be seen, for example, from the frequency-temperature relation calculated by Das<sup>6</sup> from line width measurements for methyl chloroform ( $\text{CH}_3\text{-CCl}_3$ ) conducted by Powles and Gutowsky<sup>7</sup> as early as 1953. It is clear that the  $\log \nu$  vs.  $1/T$  graph is curvilinear over the region studied. Such deviations from Arrhenius behavior have been correlated with rotational quantum mechanical (QM) tunneling of methyl groups in these materials at low temperatures.

Rotational QM tunneling of methyl groups has been treated from a theoretical point of view by Das<sup>6</sup> in 1957 and Stejskal and Gutowsky<sup>8</sup> in 1958 and more recently by Apaydin and Clough,<sup>9</sup> Davidson and Miyagawa,<sup>10</sup> Bloom,<sup>11</sup> Allen,<sup>12</sup> Huller

and Kroll,<sup>13</sup> and Johnson and Mottley,<sup>14</sup> Stejskal and Gutowsky, whose theory is most relevant to the present investigation, calculated the average tunneling frequency  $\nu_t$  as a function of temperature for barrier heights  $V_0$  in the range of 2.36 to 7.92 kcal/mol, for a methyl group attached to a rigid framework, assuming a potential of the form

$$V = \frac{1}{2}V_0(1 + \cos 3\phi) \quad (2)$$

where  $\phi$  is the angle of rotation of the methyl group. The theoretical curves predict that, at high temperatures, or in the absence of tunneling, the frequency obeys an Arrhenius temperature dependence, while at low temperatures, in the presence of tunneling, it levels off, ultimately becoming independent of temperature. A wide range of experimental NMR results is in general agreement with this hypothesis;<sup>6,15–19</sup> the line width results of Odajima, Woodward, and Sauer<sup>15</sup> and Kosfeld and von Mylius<sup>18</sup> are of special interest to this study, since they demonstrate a leveling-off of the correlation frequency of methyl motion in poly(methyl methacrylate) (PMMA) with decreasing temperature, which is indicative of QM tunneling. It should be added, however, that at very low temperatures (less than  $\sim 40$  K) an upswing in frequency with decreasing temperature has been predicted<sup>12</sup> and that certain experiments<sup>19,20</sup> appear consistent with this. However, this temperature region is far below that of the present investigation, so that an effect of this type is not likely to be encountered.

Evidence that methyl groups are indeed capable of rotational tunneling at low temperatures has also emerged from several other types of experiments on methyl-containing materials. Among the most recent are studies of electron spin resonance<sup>10,20–24</sup> and electron nuclear double resonance.<sup>25</sup>

In 1969, it was proposed that methyl rotational tunneling could be involved in viscoelastic relaxation,<sup>26</sup> the basis for this suggestion being the existence of low-temperature mechanical loss peaks in methyl-containing polymers at temperatures too low to be explained by the classical approach. The proposal made use of Stejskal and Gutowsky's theoretical treatment.<sup>8</sup> Application of the QM hypothesis to the observed dispersions led to quite reasonable estimates of the barrier heights for the different methyl groups based on structural considerations. A more detailed mechanistic picture supporting the tunneling involvement was later given.<sup>27</sup>

The proposed connection between methyl group tunneling and viscoelasticity was not, however, universally accepted. Tanabe et al.,<sup>28</sup> who detected small mechanical relaxations in ultrasonic tests on several methyl-containing polymers, concluded that methyl group motion did lead to mechanical relaxation but that QM tunneling was ineffective in that context. Sauer<sup>29</sup> has noted, however, that the general pattern followed by methyl motions is intermediate to that predicted by classical and tunneling theories and suggests that quantum effects will be manifest at very low temperatures. Golub' and Perepechko<sup>30</sup> have in fact interpreted their low-temperature ultrasonic velocity measurements on PMMA in terms of QM tunneling. Additional support for the hypothesis has arisen from the neutron incoherent inelastic scattering studies of Allen and co-workers,<sup>31,32</sup> who calculated the barriers to rotation of the  $\alpha$ -methyl group in syndiotactic and isotactic PMMA from measured fundamental torsional frequencies of the group; the barrier heights were more in agreement with the tunneling hypothesis than with thermal activation.

For several systems devoid of methyl groups, tunneling has been connected with viscoelastic and dielectric relaxation: Jäckle<sup>33</sup> has proposed a tunneling-related relaxation absorption to explain ultrasonic attenuation at very low temperatures in fused silica; Yano et al.<sup>34</sup> have interpreted the dielectric loss of polyethylene below 4.2 K in terms of phonon-assisted tunneling of hydroxyl group protons. Halperin<sup>35</sup>

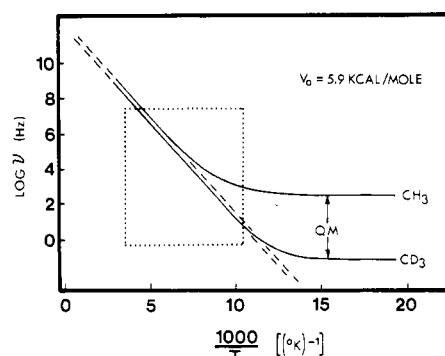


**Figure 1.** Theoretical frequency-temperature relations for methyl and deuteriomethyl reorientations by classical rotation and quantum mechanical tunneling for a barrier height of 5.9 kcal/mol. The dashed lines represent the classical case and the area enclosed by the dotted lines is the region accessible by the experimental techniques used here.

has also pointed out that "tunneling-level pairs" can qualitatively explain the anomalous thermal properties of glasses at low temperatures.<sup>36</sup> It is also interesting to note that a quantum tunneling theory of the low-temperature fracture process of polymers has been proposed.<sup>37</sup>

Existing literature data on mechanical relaxations of methyl groups in polymers<sup>38,39</sup> has, however, proved insufficient to distinguish between tunneling and thermal activation. Even the occurrence of methyl peaks is surprising, since methyl rotation under a symmetrical threefold potential (the form given by eq 2) is not expected to result in mechanical loss.<sup>38</sup> Nevertheless several mechanical peaks have been ascribed to methyl groups.<sup>29,40,41</sup>

This paper describes an attempt to resolve the question of the involvement of methyl tunneling in viscoelastic relaxation. For this purpose, an experimental examination of the  $\gamma$  relaxation in poly(methyl methacrylate) (PMMA) was launched. This relaxation was chosen since it had been identified as due to rotational motion of the backbone methyl group<sup>28,39,42,43</sup> and is experimentally accessible in convenient frequency and temperature regions. Of great importance to this investigation is the effect of isotopic substitution on tunneling, which is well known. In particular, the influence of deuteration on the rotational tunneling frequencies of methyl groups was examined by S. Reich;<sup>44</sup> his calculation (based on the theory of Stejskal and Gutowsky<sup>8</sup>) showed that deuteration should lead to only very minor changes in the classical region, while producing a profound shift to lower frequency in the tunneling region. This is illustrated in Figure 1 for methyl and deuteriomethyl groups in a potential well of 5.9 kcal/mol.

Two features apparent in Figure 1 provide the basis for this experimental study. First, if the temperature dependence of the viscoelastic energy dissipation peak is of the Arrhenius type over the entire range, then tunneling is unlikely, while a leveling-off would support tunneling. Our accessible frequency-temperature region (shown as the area enclosed by the dotted lines in Figure 1) indicates that this leveling-off, if present, should be seen for the nondeuterated polymer.

The second feature which can be investigated is the isotope effect. If it were shown that the behavior of the material containing deuteriomethyls is very close to that of the nondeuterated analogue, then tunneling would be excluded, while the presence of an isotope effect of the type shown in Figure 1 would prove that tunneling is indeed involved in viscoelastic relaxation. It should be emphasized that these criteria are based on the assumption that the theory of Stejskal and Gutowsky is valid in its essential features in its description of the tunneling process.

**Table I**  
Areas of Backbone Methyl NMR Peaks and Densities of PMMA Samples

Polymer type	<i>a</i>	Content of triads		
		% iso	% hetero	% syndio
Free-radical PMMA- <i>h</i> <sub>8</sub>	1.18	8	37	55
"Syndiotactic" PMMA- <i>h</i> <sub>8</sub>	1.16	6	32	62
Isotactic PMMA- <i>h</i> <sub>8</sub>	1.22	93	7	
Free-radical PMMA- <i>d</i> <sub>8</sub>	1.28			

<sup>a</sup> Density of molded samples, g/cm<sup>3</sup>.

### B. Literature Review of Molecular Motions in PMMA.

As a material of great commercial importance, PMMA has been much studied by dynamic mechanical, dielectric, and NMR techniques.<sup>15,18,28,38-40,45</sup> A transition map containing these literature data show, with decreasing temperature, the glass transition relaxation ( $\alpha$ ), the ester side group motion ( $\beta$ ), and a dispersion due to water impurity (H<sub>2</sub>O). All of the points at still lower temperatures are ascribed to motion of backbone methyl groups ( $\gamma$ ), except for points in the vicinity of  $1000/T \approx 13$  and  $\nu \approx 10^8$  Hz, which are attributed to the side chain or ester methyl group ( $\delta$ ). The data for the low-temperature dispersions (H<sub>2</sub>O,  $\gamma$ ), along with those obtained in this work, are shown in the results section below.

The methyl motions are interpreted as rotations of the group and, as such, are not expected to be dielectrically active. This appears to be confirmed by the absence of dielectric data for the methyl regions of the transition map. It can be seen that previous literature data for the backbone methyl (or  $\gamma$ ) relaxation are very scattered; there have been few mechanical values, and the NMR information has been limited to fairly high frequencies, greater than about  $10^3$  Hz. From previous results, it has been difficult to draw any conclusions insofar as the mechanism of this relaxation is concerned.

## II. Experimental Techniques and Results

**A. Sample Preparation and Characterization by High-Resolution NMR.** PMMA-*h*<sub>8</sub> and its fully deuterated analogue, PMMA-*d*<sub>8</sub>, were prepared as described in the previous paper.<sup>1</sup> Commercial MMA-*h*<sub>8</sub> was purified by extraction with aqueous NaOH and bulk polymerized by the free-radical method using azobis(isobutyronitrile) as initiator after several freeze/thaw cycles under vacuum to remove dissolved oxygen. The deuterated monomer was synthesized (in collaboration with Dr. E. Shohamy) using the modified acetone cyanohydrin process<sup>46</sup> and polymerized as above. Samples of isotactic and syndiotactic PMMA-*h*<sub>8</sub> were kindly supplied by Dr. B. Ginsburg, Rohm and Haas. Polymer specimens were prepared by compression molding at about 20 °C above their  $T_g$ 's of  $\sim 45$ ,  $\sim 105$ , and  $\sim 120$  °C for isotactic, free-radical, and syndiotactic PMMA, respectively.<sup>47</sup>

The tacticity of PMMA-*h*<sub>8</sub> samples can be determined by high-resolution proton NMR studies of the backbone methyl absorption.<sup>48,49</sup> Typically, three closely spaced peaks are found at a chemical shift of about 1 ppm; these correspond to syndiotactic, heterotactic, and isotactic triads in order of increasing chemical shift. The polymers used in this study were tested at 100 MHz in methylene chloride solution (8.0% weight/volume) at 30 °C, CH<sub>2</sub>Cl<sub>2</sub> having been selected as solvent since it gives better separation of the three backbone methyl peaks than do other solvents.<sup>50</sup> A Varian HA-100 spectrometer was utilized. The syndiotactic methyl peak was found at  $\sim 0.9$  ppm, the heterotactic at  $\sim 1.1$  ppm, and the isotactic at  $\sim 1.25$  ppm. The relative percentages of the three tactic species as calculated from peak areas are given in Table I below, along with the densities (at room temperature) of the molded samples.

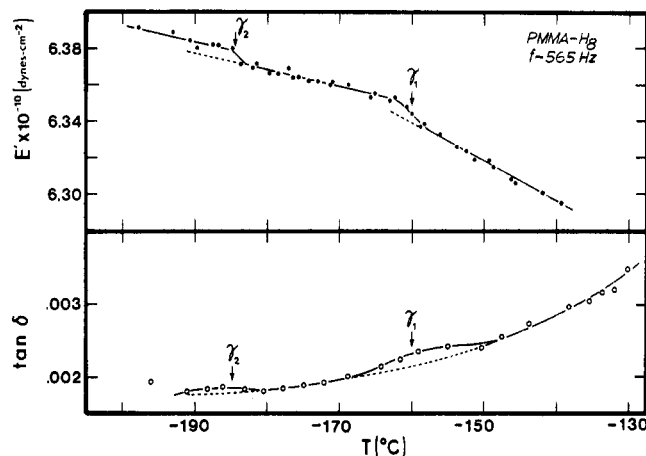


**Figure 2.** Experimental vibrating reed curves of  $E'$  and  $\tan \delta$  vs. temperature for free-radical PMMA-*h*<sub>8</sub> at  $\sim 565$  Hz.

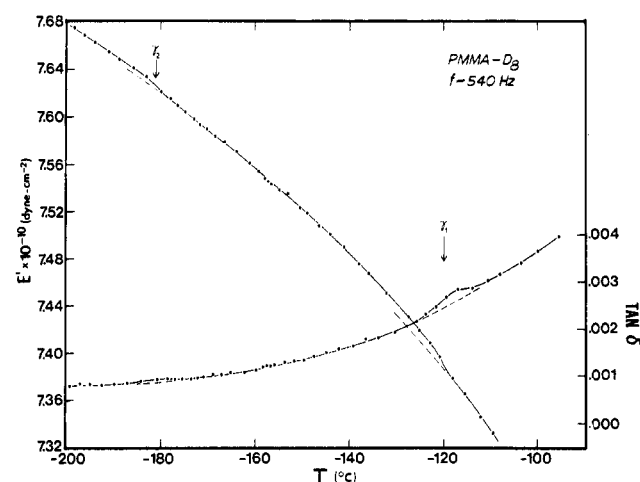


**Figure 3.** Experimental vibrating reed curves of  $E'$  and  $\tan \delta$  vs. temperature for free-radical PMMA-*d*<sub>8</sub> at  $\sim 540$  Hz.

From Table I it is evident that the free-radically polymerized PMMA-*h*<sub>8</sub> used in this study contains mainly syndiotactic and heterotactic triads in an approximate ratio of 3 to 2, which is generally found for free-radical PMMA. (This ratio may be assumed to hold for the PMMA-*d*<sub>8</sub>, which was polymerized in the same way as the free-radical PMMA-*h*<sub>8</sub>.) The "syndiotactic" PMMA-*h*<sub>8</sub> is similar to the free-radical PMMA, except that it has a higher syndiotactic to heterotactic ratio of about 2 to 1. The isotactic sample consists almost entirely of isotactic triads.

**B. Dynamic Mechanical Test Instruments.** Both PMMA-*h*<sub>8</sub> and its fully deuterated analogue (PMMA-*d*<sub>8</sub>) were investigated using a free vibration torsional pendulum with a frequency range of 0.2 to 10 Hz, a high-precision vibrating reed device operating in the frequency region  $2 \times 10^2$  to  $2 \times 10^4$  Hz, and an ultrasonic apparatus employing the single crystal pulse echo technique over the  $10^6$  to  $10^8$  Hz region. The loss tangent and modulus were measured as a function of temperature at approximately constant frequency, over the ranges of the three instruments, using liquid nitrogen as coolant.

The torsional pendulum was of the inverted type and has been described previously in detail.<sup>51</sup> The real and imaginary shear moduli ( $G'$  and  $G''$  respectively) and corrected loss tangent ( $\tan \delta_c$ ) were calculated from the appropriate equations.<sup>52</sup> In order to attain the high precision in  $G'$  necessary to detect very low strength relaxations, accurate measure-

**Table II**  
**Summary of Vibrating Reed Experimental Data for the  $\gamma$  Relaxation Region of Free-Radical PMMA- $h_8$  and PMMA- $d_8$**

Polymer	Relaxation position			Relaxation strength $\Delta E'/E'(\times 10^{-3})$	Tan $\delta$ peak height ( $\times 10^{-4}$ )	Exptl conditions		
	$\nu$ , Hz <sup>a</sup> ( $\gamma_1$ or $\gamma_2$ )	$T$ , °C $\gamma_1$	$T$ , °C $\gamma_2$			Warm rate, °C/h	Pressure, cm Hg	Vibration mode <sup>b</sup>
PMMA- $h_8$	225.3		-200.5	1.0		8	1.4	f
	274	-162.		0.9		7	1.3	f
	277		-198		~1	7	1.3	f
	295.3		-196.5	0.5		10	3.0	f
	496	-167.5		0.6		21	2.0	f
	497	-170		0.6	~0.8	~41	2.0	f
	499		-190		~0.7	~50	2.0	f
	565	-160		1.5	~2	~30	2.75	f
	566		-184	0.9	~1	~30	2.75	f
	568	-156		1.8		16	1.35	f
	569.5	-162.5		0.9		7	1.3	f
	571		-188	0.6		7	1.3	f
	710	-145		1.4		11	1.3	f
	712.5	-151		0.8	~0.5	6	1.2	f
	1322		-179.5	0.6		7	1.3	1
	1633		-179		~1.5	8	1.3	1
	1761	-147		1.1		9	2.0	1
	1770		-175	0.6		10	3.0	1
	3025	-118		0.9		14	2.0	1
	3025	-117		0.9		10	2.0	1
	3036	-121		0.8		26	2.0	1
	4319	-125		1.7		12	1.3	1
	4379		-172.5	0.9		10	1.3	1
	9105	-116		2.0		12	1.3	2
	9243		-164	0.9		7	1.3	2
PMMA- $d_8$	368	-119		1.7	7.5	~10	2.5	f
	540.5	-120		1.1	2	8	1.4	f
	538.5	-120		1.2	2	15	2.0	f
	547		-181	0.6	0.7	15	2.3	f
	1007	-118		1.1	1.6	12	2.0	f
	1019		-175	0.7		~30	2.0	f
	1392	-119		1.2		~11	1.4	1
	1416		-176	0.8		9	1.4	1
	1731	-118.5		1.0	2	10	1.4	f
	3934	-106		~1.3	~10	12	1.4	2
	4015		-175	1.0	1.5	9	1.4	2

<sup>a</sup> Brackets indicate results from the same run. <sup>b</sup> f = fundamental; 1 = first overtone; 2 = second overtone.

ments of oscillation periods were performed; at each temperature, the decay was allowed to proceed until oscillations were no longer well defined (which depends on the magnitude of  $\tan \delta$  and on the noise level), and the time corresponding to a large number of cycles was measured directly from the chart. For PMMA- $d_8$ , at temperatures less than ca. -150 °C, 400 cycles could be counted in this way, leading to a precision in  $G'$  approaching 1 part in 1000. Accuracy in  $\tan \delta$  was obtained by measuring every 20th oscillation amplitude and least-squares fitting this data (corrected for noise) to yield the logarithmic decrement.

The vibrating reed instrument adopted for this study was a high-precision device employing a piezoelectric detection technique, based on the design of Fielding–Russell and Wetton.<sup>53</sup> A lower frequency vibrating reed with a novel optical detection technique<sup>54</sup> and an acoustic spectrometer based on the design of Schlein and Shen<sup>55</sup> also saw some limited use. An electronic frequency counter was incorporated into the Fielding–Russell and Wetton design, allowing measurement of the resonant frequency to approximately 1 part in 50 000 for polymer samples at low temperatures (where  $\tan \delta \sim 0.001$ ). This permitted the calculation of the Young's modulus  $E'$  with a precision of better than 1 part in  $10^4$ , enabling the detection of the small methyl dispersion. It should be emphasized, however, that the absolute accuracy of the measurements is obviously much less than that number.

The ultrasonic apparatus allowed measurement of atten-

uation coefficient and speed of sound for longitudinal waves in specimens with  $\tan \delta$  less than ~0.02 over a frequency range of 1 to 20 MHz. In the single crystal pulse echo technique, a piezoelectric transducer is used both to generate an initial ultrasonic pulse which is coupled into a sample and to detect echoes from the opposite face of the sample; an exponentially decaying series of evenly spaced pulses may be observed on an oscilloscope. An essential feature of the test was the selection of a Tektronix 535A oscilloscope operated in the "A delayed by B" mode.<sup>56</sup> This permitted very accurate measurement of the time between successive ultrasonic echoes, which, in conjunction with measurements of relative attenuation levels (obtained by means of a stepped attenuator accurate to 0.1 dB in 70 dB), led to sufficient precision in  $\tan \delta$  to enable observation of methyl relaxations.

**C. Vibrating Reed Results.** In view of the fact that the proof of a QM tunneling involvement in methyl relaxation hinges primarily on the vibrating reed results, these are presented first. A large body of data was obtained on the vibrating reed apparatus for PMMA- $h_8$  and PMMA- $d_8$  prepared by free-radical polymerization, over the frequency region of ~230 to ~9250 Hz, achieved through the use of fundamental and overtone vibration frequencies. The real Young's modulus  $E'$  and (in some cases)  $\tan \delta$  have been measured as a function of temperature, covering the region from ca. -200 to ca. -100 °C. Experimentally, samples were warmed from pumped liquid nitrogen temperature under partial vacuum (pressure

Table III  
Average Relaxation Strengths for  $\gamma$  Relaxations in Free-Radical PMMA- $h_8$  and PMMA- $d_8$

Polymer	$\gamma_1$ relaxation strength ( $\Delta E'/E' \times 10^3$ )			$\gamma_2$ relaxation strength ( $\Delta E'/E' \times 10^3$ )		
	Av	Std. dev	No. of obs	Av	Std. dev	No. of obs
PMMA- $h_8$	1.14	0.46	14	0.75	0.19	8
PMMA- $d_8$	1.23	0.23	7	0.78	0.17	4

Table IV  
Summary of Acoustic Experimental Data for the "Water" Relaxation Region of Free-Radical PMMA- $h_8$

Relaxation position $\nu$ , Hz	Relaxation strength $\Delta E'/E'$	Tan $\delta$ peak height	Exptl conditions		Pressure, cm Hg
			Type of apparatus	Warm or cool rate, $^{\circ}\text{C}/\text{h}$	
269		0.0015	Vibrating reed-optical	Not recorded (warming)	~1
1075	0.020		Vibrating reed-piezoelectric	~50 (cooling)	76
1365	0.032		Acoustic spectrometer	~80 (cooling)	76

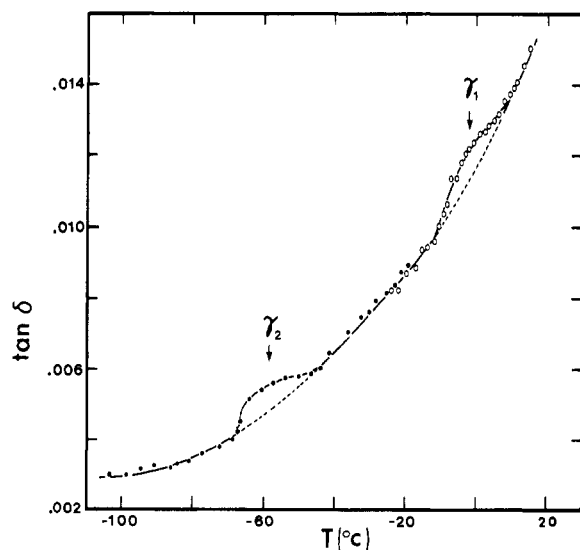


Figure 4. Ultrasonic data showing  $\tan \delta$  vs. temperature for free-radical PMMA- $d_8$  at 13.4 MHz. (Results of two separate experiments at that frequency are shown.)

~2 cm Hg) at warming rates varying from ~10  $^{\circ}\text{C}/\text{h}$  (the usual case) to ~50  $^{\circ}\text{C}/\text{h}$ . Under these conditions, using the high-precision instrument previously described, very low strength mechanical relaxations were detected. Two such relaxations, denoted  $\gamma_1$  and  $\gamma_2$  in order of decreasing temperature location, are evident from the data, generally as inflections in modulus, and sometimes as peaks in  $\tan \delta$ . Figure 2 shows data from one such run obtained on the vibrating reed apparatus for PMMA- $h_8$  at a frequency of ~565 Hz, while Figure 3 shows corresponding data for PMMA- $d_8$  at ~540 Hz. Both of these figures show the  $\gamma$  relaxations as inflections in modulus and also as  $\tan \delta$  peaks. This was not always the case, however; often  $\tan \delta$  curves showed too much scatter to permit detection of small peaks. Nevertheless, inflections were almost always observed in the modulus. The frequency and temperature positions of all the low-temperature  $\gamma$  relaxations found in the vibrating reed tests are summarized in Table II, along with relevant experimental quantities. These data show that peak positions are quite reproducible.

For PMMA- $h_8$ , the average relaxation strength ( $\Delta E'/E'$ ) of the  $\gamma_1$  relaxation is  $1.1 \times 10^{-3}$  while that of the  $\gamma_2$  dispersion is  $0.75 \times 10^{-3}$ . Where observed,  $\tan \delta$  peak heights are of the order of  $1 \times 10^{-4}$ . The average  $\gamma_1$  and  $\gamma_2$  relaxation strengths for PMMA- $d_8$  are similar:  $1.2 \times 10^{-3}$  and  $0.78 \times 10^{-3}$ , respectively. Here, however,  $\tan \delta$  peak heights are of the order

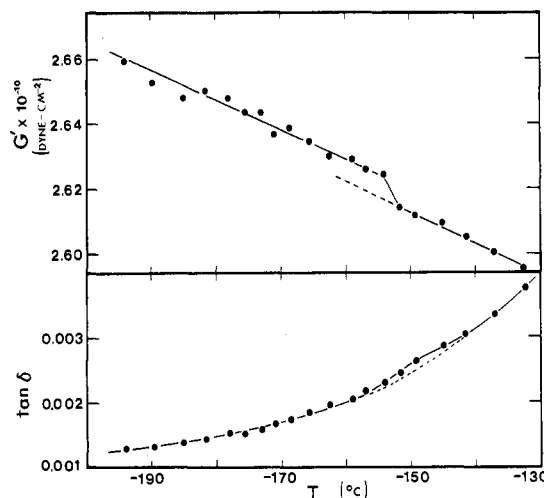


Figure 5. Torsional pendulum curves of  $G'$  and  $\tan \delta$  vs. temperature for free-radical PMMA- $d_8$  at ~2.35 Hz.

of  $2 \times 10^{-4}$ . The reason for the difference in the  $\tan \delta$  peak heights is, conceivably, the lower precision of these measurements. The  $\gamma$  relaxation strengths are summarized along with their standard deviations in Table III below.

Several preliminary vibration tests revealed dispersion at temperatures greater than  $-10^{\circ}\text{C}$  for PMMA- $h_8$  samples which had been exposed to moisture. These results are summarized in Table IV. It should be noted that the three sets of data were obtained on three different vibration instruments, which have previously been briefly described. This "water" relaxation has a strength of ~0.025 with a  $\tan \delta$  peak height of ~0.0015.

Although considerable care was taken to keep subsequent PMMA samples free of moisture, it was difficult to exclude water completely as indicated by more recent ultrasonic tests on free-radical PMMA- $h_8$ , which still contain a hint of the "water" dispersion.

**D. Ultrasonic Results.** Ultrasonic tests were performed on the PMMA samples using the single-crystal pulse echo technique described in the experimental section. The free-radical PMMA- $h_8$  was investigated at several frequencies from 1.3 to 20.0 MHz, while free-radical PMMA- $d_8$  and both isotactic and "syndiotactic" PMMA- $h_8$  were tested at ~13.5 MHz only, for comparison purposes. Mechanical relaxations were detected either as shoulders in  $\tan \delta$  vs. temperature curves, as inflections in the velocity/temperature curve, or as local minima in the dB level of a single echo.

Corresponding to the vibrating reed tests, very small me-

Table V  
Summary of Ultrasonic Data Obtained for PMMA Samples of Various Composition and Tacticity<sup>a</sup>

Material	Relaxation position					Relaxation strength $\Delta v/v$ ( $\times 10^{-3}$ )	Tan $\delta$ peak height ( $\times 10^{-4}$ )	Warming or cooling rate, °C/h
	$\nu$ , MHz	$T_{\gamma_1}$ , °C	$T_{\gamma_2}$ , °C	$T_{\gamma_3}$ , °C	$T_{H_2O}$ , °C			
PMMA- $h_8$ (free radical)	1.3				+6	2	3	25 (cool)
	1.3	-38				2	4	25 (cool)
	3.4	-22				2	5	35 (warm)
	8.4	-10				2	4	30 (warm)
	12.9 <sup>b</sup>		-56			2	3	25 (cool)
	13.6				+34		(~4) <sup>c</sup>	25 (warm)
	13.6	-1					4	12 (warm)
	18.5				+42		(~2)	30 (warm)
	18.5			(-92.5)			~1	30 (warm)
	20.0	-1					(~5) <sup>c</sup>	35 (warm)
PMMA- $d_8$ (free radical)	13.4	-2					10	25 (warm)
	13.4		-58				7	50 (warm)
PMMA- $h_8$ (isotactic)	13.7			-97		3	4	30 (cool)
PMMA- $h_8$ ("syndiotactic")	13.5	-16				8	7	35 (warm)
	13.5		-56			11	6	35 (warm)

<sup>a</sup> The sample-to-transducer bonding agent was nonaqueous cement, unless otherwise noted. <sup>b</sup> Bonding agent = 3-chloropropylbenzene. A peak thought due to bonding agent was observed at -85 °C. <sup>c</sup> Estimated from local minimum in dB curve for a single echo.

Table VI  
Summary of Torsional Pendulum Data Obtained for Deuterated PMMA Samples

Material	Relaxation position		Relaxation type	Relaxation strength $\Delta G'/G'$ ( $\times 10^{-3}$ )	Tan $\delta$ peak heights ( $\times 10^{-4}$ )
	$\nu$ , Hz	$T$ , °C			
PMMA- $d_8$ (free radical)	0.75	-157	$\gamma_1$	1.5	~1
	2.35	-153	$\gamma_1$	2	~1

chanical dispersions were detected in the temperature interval from -10 to +50 °C. In two samples, as many as four relaxations (denoted  $H_2O$ ,  $\gamma_1$ ,  $\gamma_2$ , and  $\gamma_3$  in order of decreasing temperature) were observed in the PMMA's. Figure 4 shows a representative ultrasonic curve of  $\tan \delta$  vs. temperature for free-radical PMMA- $d_8$  at 13.4 MHz which illustrates the  $\gamma_1$  and  $\gamma_2$  relaxations. A summary of the ultrasonic data obtained is given as Table V. In most of the experiments, warming (or cooling) rates of ~30 °C/h were employed, with nonaqueous cement as the sample-to-transducer bonding agent.

**E. Torsional Pendulum Results.** The torsional pendulum technique which has already been described in the experimental section was applied to PMMA- $d_8$  samples in a nitrogen atmosphere at two frequencies; one result is given in Figure 5. The  $G'$  curve provides evidence of a very low strength relaxation near -153 °C at 2.35 Hz; the  $\tan \delta$  curve also hints at the presence of a dispersion in this region. Despite the low warming rate of 15 to 20 °C/h employed for these tests, a sizable temperature gradient of ~10 °C at -150 °C existed inside the sample chamber. This must contribute toward limiting the size of mechanical dispersion observable in the test.

An experiment on PMMA- $h_8$  at 2.35 Hz over the same temperature region as above was also attempted, but results were too scattered to observe a relaxation even if one were present. In this case, due to a higher  $\tan \delta$ , only 260 cycles could be counted, leading to reduced accuracy in the period measurement (as many as 400 cycles were counted for PMMA- $d_8$ ).

The relaxations observed in these torsional pendulum tests are summarized in Table VI below.

### III. Discussion

**A. Demonstration of Methyl Group Tunneling.** The experimental frequency-temperature positions of those dynamic mechanical methyl relaxations labeled  $\gamma_1$  have been plotted in Figure 6 for both PMMA- $h_8$  and PMMA- $d_8$ . The dashed lines represent calculations from the theory of Stejskal

and Gutowsky<sup>8</sup> for methyl rotations over barriers of 6.4, 6.9, and 7.4 kcal/mol. This figure shows clearly that both criteria for tunneling are met, i.e., that  $\log \nu$  vs.  $1/T$  is non-Arrhenius for the nondeuterated polymer, tending to level off at low temperatures, and that a  $CH_3/CD_3$  isotope effect also exists, the deuterated polymer following a linear Arrhenius-type relation over the whole frequency/temperature range studied. It can be seen that the behavior for PMMA- $h_8$  is of the type predicted by the tunneling theory but that the agreement is only qualitative. This may be due to the fact, noted by Ingold,<sup>57</sup> that a slight change in the shape of the potential barrier can result in significant changes in the  $\log \nu$  vs.  $1/T$  plot. Thus, from the shape of the curves and from the presence of the isotope effect, it can be concluded that tunneling of methyl groups is indeed involved in viscoelastic relaxation if the theory of Stejskal and Gutowsky is correct in its essential features. The present study represents the first observation of an isotope effect in the field of viscoelastic properties of polymers.

**B. Tacticity Effect in PMMA.** Figure 7 contains the complete transition map for PMMA, showing both literature data (open symbols) and the relaxations observed in the present study (filled symbols, Tables II and IV–VI). Two NMR literature points for isotactic PMMA- $h_8$ <sup>58,59</sup> have also been included. For simplicity, the  $\alpha$  and  $\beta$  relaxations are shown only as lines.

Figure 7 clearly shows that two separate relaxations are occurring in the backbone methyl region of free-radical PMMA: they are labeled  $\gamma_1$  and  $\gamma_2$  in order of decreasing temperature and have activation energies of 6.7 and 3.3 kcal/mol; they may be assigned to reorientations of syndiotactic and heterotactic backbone methyl groups, respectively. This interpretation is suggested by the high-resolution NMR data (Table I) which indicated a syndiotactic to heterotactic triad number ratio of about 3 to 2, in close agreement with the average ratio of relaxation strengths found in the vibrating reed studies (1.5 for PMMA- $h_8$  samples and 1.6 for PMMA- $d_8$

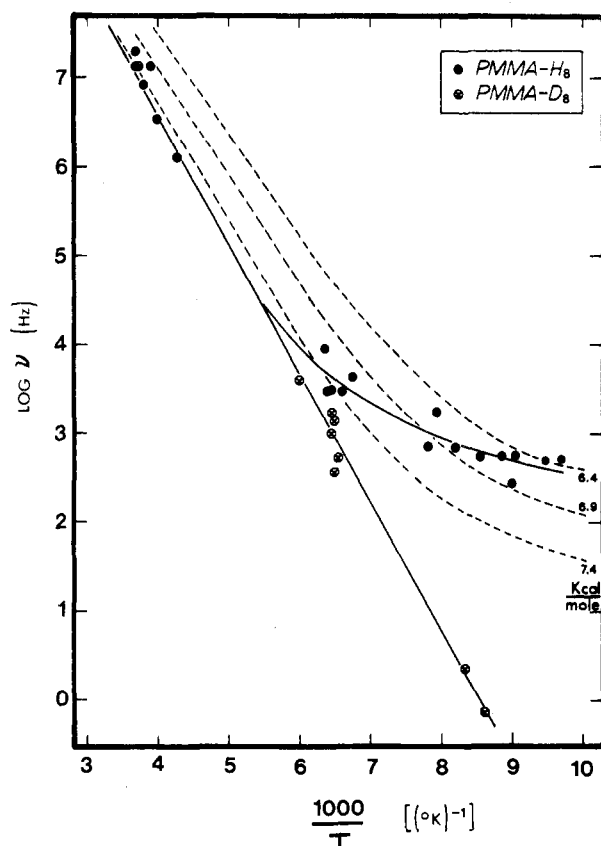


Figure 6. Experimental frequency-temperature map for the  $\gamma_1$  relaxation in PMMA- $h_8$  and PMMA- $d_8$ . (The region covered by the graph corresponds to that outlined in dots on Figure 1.) The dashed lines represent calculations from the theory of Stejskal and Gutowsky<sup>8</sup> for barrier heights of 6.4, 6.9, and 7.4 kcal/mol.

samples). It is doubtful whether the lower temperature  $\gamma_2$  relaxation can be ascribed to isotactic groups because very little (<10%) isotactic material is present in the free-radical polymer.

The  $\log \nu$  vs.  $1/T$  plot of the  $\gamma_2$  relaxation, here assigned to heterotactic backbone methyls, shows the beginnings of the curvature and  $\text{CH}_3/\text{CD}_3$  isotope effect indicative of QM rotational tunneling, but measurements need to be extended to lower frequencies and temperatures for confirmation.

It should be noted that the two NMR literature points for isotactic PMMA given in Figure 7 are close to the  $\gamma_2$  relaxation of this work. It is conceivable that both the heterotactic and isotactic dispersions occur in the same temperature region. However, the high-frequency (ca.  $10^7$  Hz) isotactic peaks from this study (labeled  $\gamma_3$ ) lie at a somewhat lower temperature than that for the isotactic sample quoted in the literature. Since those previous workers have not had pure isotactic material (their polymers are only stated as containing <24% atactic material), they may possibly have determined the heterotactic peak.

**C. High-Temperature Projection.** If the straight lines obtained in Figure 7 are extrapolated to higher frequencies and temperatures, a striking feature is evident: all the relaxations appear to project through a region (or perhaps a single point) near  $\log \nu \sim 9$  and  $T \sim 200^\circ\text{C}$ . This pattern for PMMA is remarkably similar to that observed in 1968 by Starkweather<sup>60</sup> for several semicrystalline polymers; there, the  $\log(\nu/T)$  vs.  $1/T$  plots for the mechanical relaxations often converged at the crystalline melting point,  $T_m$ . Similar observations have been made informally for noncrystalline polymers by several investigators, but, except for the work of G. D. Patterson discussed below, no literature references could be

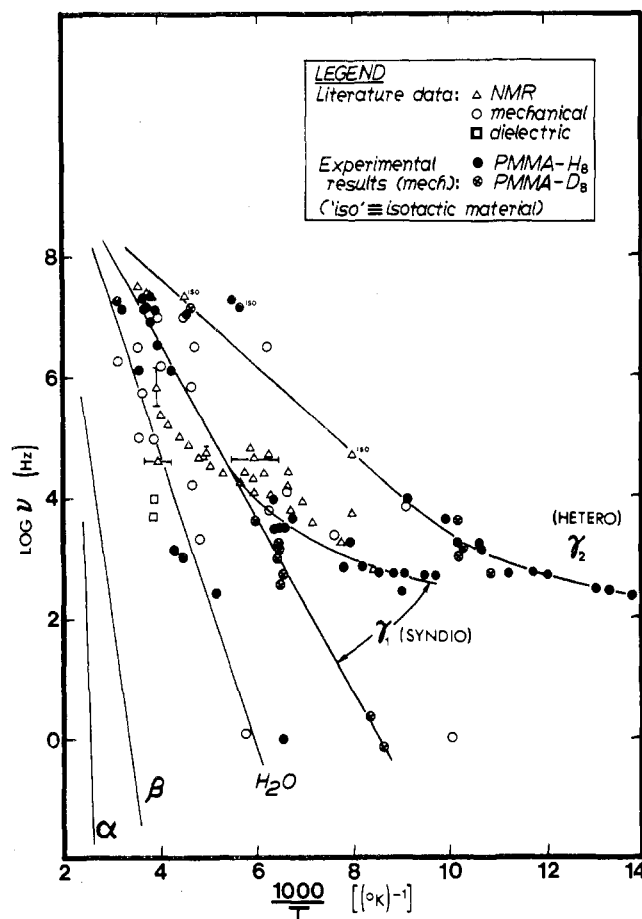


Figure 7. The transition map for PMMA, showing the experimental results in conjunction with previous literature data. (The  $\alpha$  and  $\beta$  relaxations are shown only as lines, for simplicity.)

found. The intersection of the various molecular motions at a finite frequency and temperature may well be a general feature for amorphous polymers. The well-known merging at high temperatures and frequencies of the main chain ( $\alpha$ ) and secondary ( $\beta$ ) relaxations certainly supports this concept. In recent Brillouin scattering studies, G. D. Patterson<sup>61</sup> observed just one loss maximum in several amorphous polymers at frequencies near  $10^{9.5}$  Hz, in agreement with this merging of dispersions. He also demonstrated that the temperatures of maximum loss lay on extrapolations of the secondary  $\beta$  relaxations for poly(methyl acrylate), poly(isobutylene), atactic poly(propylene), and poly(vinyl acetate) and concluded that, at high temperatures, the  $\beta$  dispersion line extends, while the  $\alpha$  merges with it.

#### IV. Summary

In summary, dynamic mechanical experiments have indicated that both a pronounced curvature in the  $\log \nu$  vs.  $1/T$  plot and a large deuteration effect are observed for the  $\gamma_1$  relaxation in free-radical PMMA, in qualitative agreement with the methyl group tunneling theory of Stejskal and Gutowsky.<sup>8</sup> If this theory is indeed valid then rotational QM tunneling of methyl groups is involved in viscoelastic relaxation.

It was also shown that the  $\gamma$  relaxation of PMMA is a function of the tacticity of the polymer, with two distinct dispersions (labeled  $\gamma_1$  and  $\gamma_2$ ) detected for the free-radically prepared polymers; these had activation energies of 6.7 and 3.3 kcal/mol, respectively. The  $\gamma_1$  relaxation was ascribed to syndiotactic backbone methyls and the  $\gamma_2$  to heterotactic groups. Some evidence of a third related relaxation (labeled

$\gamma_3$ ) was found; it is possible that this peak may correspond to isotactic material, although the evidence for this is weak. Finally, comparison of experimental and literature data for all the viscoelastic relaxations in PMMA suggests that the transitions all converge at  $\sim 200^\circ\text{C}$  and  $10^9\text{ Hz}$ .

**Acknowledgments.** It is a pleasure to acknowledge the benefit of the advice of Dr. J. Krause of Bell Laboratories in the construction of the ultrasonic instrument used in this study. The isotactic and syndiotactic samples of PMMA were kindly supplied by Dr. B. Ginsburg of Rohm and Haas. One of us (J.W.) was the recipient of a J. W. McConnell Memorial Fellowship. This work was supported in part by a grant from the National Research Council of Canada, and in part by the donors of the Petroleum Research Fund, administered by the American Chemical Society.

## References and Notes

- (1) A preliminary report of this work was presented in *Phys. Rev. Lett.*, **35**, 951 (1975). The present paper is based in part on the doctoral thesis of J. Williams, McGill University, 1978.
- (2) See, for example, D. W. McCall, *Acc. Chem. Res.*, **223** (1971).
- (3) See, for example, V. J. McBrierty, *Polymer*, **15**, 503 (1974).
- (4) See, for example, K. J. Laidler, "Chemical Kinetics", McGraw-Hill, New York, N.Y., 1965.
- (5) J. Heijboer, Doctoral Dissertation, University of Leiden, 1972.
- (6) T. P. Das, *J. Chem. Phys.*, **27**, 763 (1957).
- (7) J. G. Powles and H. S. Gutowsky, *J. Chem. Phys.*, **21**, 1695 (1953).
- (8) E. O. Stejskal and H. S. Gutowsky, *J. Chem. Phys.*, **28**, 388 (1958).
- (9) F. Apaydin and S. Clough, *J. Phys. C*, **1**, 932 (1968).
- (10) R. B. Davidson and I. Miyagawa, *J. Chem. Phys.*, **52**, 1727 (1970).
- (11) M. Bloom, *Pure Appl. Chem.*, **32**, 99 (1972).
- (12) P. S. Allen, *J. Phys. C*, **7**, L 22 (1974).
- (13) A. Huller and D. M. Kroll, *J. Chem. Phys.*, **63**, 4495 (1975).
- (14) C. S. Johnson, Jr., and C. Mottley, *J. Phys. C*, **9**, 2789 (1976).
- (15) A. Odajima, A. E. Woodward, and J. A. Sauer, *J. Polym. Sci.*, **55**, 181 (1961).
- (16) C. D. Knutson and D. M. Spitzer, Jr., *J. Chem. Phys.*, **45**, 407 (1966).
- (17) J. Haupt and W. Muller-Warmuth, *Z. Naturforsch.*, **A**, **24**, 1066 (1969).
- (18) R. Kosfeld and U. von Mylius, *Kolloid-Z.*, **250**, 1081 (1972).
- (19) B. Lammel and R. Kosfeld, *Colloid Polym. Sci.*, **253**, 881 (1975).
- (20) S. Clough and J. R. Hill, *J. Phys. C*, **7**, L 20 (1974).
- (21) S. Clough and B. J. Mulady, *Phys. Rev. Lett.*, **30**, 161 (1973).
- (22) J. L. Carolan, S. Clough, N. D. McMillan, and B. Mulady, *J. Phys. C*, **5**, 631 (1972).
- (23) S. Clough, J. R. Hill, and T. Hobson, *Phys. Rev. Lett.*, **33**, 1257 (1974).
- (24) S. Clough, J. R. Hill, and F. Poldy, *J. Phys. C*, **5**, 1739 (1972).
- (25) S. Clough, J. R. Hill, and F. Poldy, *J. Phys. C*, **5**, 518 (1972).
- (26) A. Eisenberg and S. Reich, *J. Chem. Phys.*, **51**, 5706 (1969).
- (27) S. Reich and A. Eisenberg, *J. Chem. Phys.*, **53**, 2847 (1970).
- (28) Y. Tanabe, J. Hirose, K. Okano, and Y. Wada, *Polym. J.*, **1**, 107 (1970).
- (29) J. A. Sauer, *J. Polym. Sci., Part C*, **32**, 69 (1971).
- (30) P. D. Golub' and I. I. Perepechko, *Sov. Phys.-Acoust. (Engl. Transl.)*, **19**, 391 (1974).
- (31) J. S. Higgins, G. Allen, and P. N. Brier, *Polymer*, **13**, 157 (1972).
- (32) G. Allen, C. J. Wright, and J. S. Higgins, *Polymer*, **15**, 319 (1974).
- (33) J. Jäcke, *Z. Phys.*, **257**, 212 (1972).
- (34) O. Yano, K. Saiki, S. Tarucha, and Y. Wada, *J. Poly. Sci., Polym. Phys.*, **15**, 43 (1977).
- (35) B. I. Halperin, *Ann. N.Y. Acad. Sci.*, **279**, 173 (1976).
- (36) See, for example, R. O. Pohl and G. L. Salinger, *Ann. N.Y. Acad. Sci.*, **279**, 150 (1976).
- (37) J. J. Gilman and H. C. Tong, *J. Appl. Phys.*, **42**, 3479 (1971).
- (38) N. G. McCrum, B. E. Read, and G. Williams, "Anelastic and Dielectric Effects in Polymeric Solids", Wiley, New York, N.Y., 1967.
- (39) D. W. McCall, *Natl. Bur. Stand. Spec. Publ.*, **301**, 475 (1969).
- (40) P. G. Bordoni, M. Nuovo, and L. Verdini, *Nuovo Cimento*, **20**, 667 (1961).
- (41) T. Kajiyama and W. J. MacKnight, *Macromolecules*, **2**, 254 (1969).
- (42) J. G. Powles, *J. Polym. Sci.*, **22**, 79 (1956).
- (43) K. M. Sinnott, *J. Polym. Sci.*, **42**, 3 (1960).
- (44) S. Reich, private communication.
- (45) R. Hayakawa et al., *Proc. Jap. Conf. Polym. Solid State*, **99** (1972).
- (46) B. Golding, "Polymers and Resins", Van Nostrand, Princeton, N.J., 1959.
- (47) W. R. Krigbaum and J. V. Dawkins in "Encyclopaedia of Polymer Science and Technology", Vol. 8, Wiley, New York, N.Y., 1968, p 764.
- (48) A. Nishioka, H. Watanabe, K. Abe, and Y. Sono, *J. Polym. Sci.*, **48**, 241 (1960).
- (49) N. W. Johnston and P. W. Kopf, *Macromolecules*, **5**, 87 (1972).
- (50) K. C. Ramey and J. Messick, *J. Polym. Sci., Part A-2*, **4**, 155 (1966).
- (51) B. Cayrol, Doctoral Thesis, McGill University, 1972.
- (52) These are presented in a number of sources and are summarized by R. Yeo, Doctoral Thesis, McGill University, 1976.
- (53) G. S. Fielding-Russell and R. E. Wetton, "Plastics and Polymers", June 1970, p 179.
- (54) S. Reich and A. Eisenberg, *Rev. Sci. Instrum.*, **41**, 1905 (1970).
- (55) H. Schlein and M. Shen, *Rev. Sci. Instrum.*, **40**, 587 (1969).
- (56) D. Y. Chung, *Rev. Sci. Instrum.*, **42**, 878 (1971).
- (57) G. Brunton, D. Griller, L. R. C. Barclay, and K. U. Ingold, *J. Am. Chem. Soc.*, **98**, 6803 (1976).
- (58) J. G. Powles, J. H. Strange, and D. J. H. Sandiford, *Polymer*, **4**, 401 (1963).
- (59) T. M. Connor and A. Hartland, *Phys. Lett.*, **23**, 662 (1966).
- (60) H. W. Starkweather, Jr., *J. Macromol. Sci., Phys.*, **2**, 781 (1968).
- (61) G. D. Patterson, *J. Polym. Sci., Polym. Phys.*, **15**, 455 (1977).

## Electric Birefringence of Dilute Suspensions of Poly(ethylene oxide) Crystals in Ethylbenzene

Ulrich Leute<sup>1</sup> and Thor L. Smith\*

IBM Research Laboratory, San Jose, California 95193. Received January 5, 1978

**ABSTRACT:** Suspensions of poly(ethylene oxide) (PEO) crystals in ethylbenzene were subjected to electric pulses, including those of rapidly reversed polarity, and to alternating fields. The time and frequency dependence of the resulting birefringence shows that crystal orientation arises from a slowly induced dipole moment, as concluded by Picot et al. from the frequency dependence of the birefringence. The effect of the finite rate of polarization on the time and frequency dependence of the birefringence is discussed in terms of an electric-relaxation time, estimated to be a few milliseconds, and the birefringence-relaxation time. The field-strength dependence of the steady-state birefringence was represented by an equation; derived by Shah, that applies to a disk-shaped particle in which a dipole moment is induced perpendicular to its unique axis. Thereby it was found that  $(\alpha_2 - \alpha_1)/L^3 \approx 2.4 \times 10^{-11} \text{ F/m}$ , where  $(\alpha_2 - \alpha_1)$  is the excess electric polarizability and  $L$  is the effective length of the square lamellar crystals. This relation agrees semiquantitatively with that obtained from a treatment by O'Konski and Krause of the excess polarizability of a conducting spheroid in a fluid. The suspensions studied were prepared by the self-seeding technique from ethylbenzene solutions of a PEO-PPO-PEO triblock copolymer (Pluronic F127), where PPO denotes atactic poly(propylene oxide). The size of the crystals, which were essentially monodisperse, was varied between 0.87 and 2.65  $\mu\text{m}$ .

When a liquid suspension of polymer crystals is subjected to an electric field, the crystals orient and the suspension thereby becomes birefringent. Following some exploratory studies,<sup>2-4</sup> Picot et al.<sup>5,6</sup> investigated suspensions of single

crystals prepared by the self-seeding technique<sup>7-10</sup> from solutions of a diblock copolymer of poly(ethylene oxide) (PEO) and polystyrene (PS) and also from solutions of PEO and polyethylene homopolymers. Because the birefringence was